Packings of a charged line on a sphere

Silas Alben*
School of Mathematics, Georgia Institute of Technology, Atlanta, Georgia 30332-0160, USA
(Received 17 June 2008; published 5 December 2008)

We find equilibrium configurations of open and closed lines of charge on a sphere, and track them with respect to varying sphere radius. Closed lines transition from a circle to a spiral-like shape through two low-wave-number bifurcations—"baseball seam" and "twist"—which minimize Coulomb energy. The spiral shape is the unique stable equilibrium of the closed line. Other unstable equilibria arise through tip-splitting events. An open line transitions smoothly from an arc of a great circle to a spiral as the sphere radius decreases. Under repulsive potentials with faster-than-Coulomb power-law decay, the spiral is tighter in initial stages of sphere shrinkage, but at later stages of shrinkage the equilibria for all repulsive potentials converge on a spiral with uniform spacing between turns. Multiple stable equilibria of the open line are observed.

DOI: 10.1103/PhysRevE.78.066603 PACS number(s): 41.20.−q, 89.75.Kd, 05.65.+b

I. INTRODUCTION

Confinement of mutually repelling units in a closed geometry is a common phenomenon in physics, chemistry, and biology [1–3], and has important structural and functional consequences for the ensemble of confined units. For example, during the packing of DNA and RNA into viral shells, interaction between individual nucleotides leads to the formation of ordered coils [4–6]. Dielectric properties of the solvent modify the interaction potential, and elastic properties of the nucleotide chains (bending and twist rigidity) also play important roles.

The stable aggregates which result from interactions through long-range potentials are studied as examples of pattern formation [7,8] and have potential uses in the spontaneous formation of new structures known as self-assembly [9–11]. One of the best-known models is the Thomson problem for the equilibria of equal Coulomb charges on a sphere [12]. Many of the equilibria which have been identified so far consist of a curved hexagonal lattice disrupted by 12 or more pentagonal defects [13]. The number of equilibria grows rapidly—perhaps exponentially—with the number of charges [14].

Recently, Slosar and Podgornik considered a variation of the Thomson problem wherein the charges are joined by rigid links into an open single-stranded chain [15]. Using simulated annealing they identified a spiral configuration as well as configurations which are locally similar to a spiral but globally disordered. Other equilibria, including disordered states, were found in simulations of aggregates of polyelectrolytes [16]. Previously, Saff and Kuijlaars had derived energy bounds for the large-number limit of point particles which repel with arbitrary power-law decay with distance [17]. They identified a "generalized spiral set" as a configuration which yields a uniform distribution of points on a sphere.

Here we extend the study of the connected-charges problem in three ways: we consider the cases of closed chains, varying sphere radius, and varying power law of repulsion. First, we determine the behavior of the self-repelling chain as a function of the radius of the confining sphere. We find that a closed chain undergoes two bifurcations as the radius shrinks, the first leading to a "baseball-seam" configuration, and the second leading to twist. Subsequently, the twist gradually increases as the chain tends to a spiral configuration. We also find a distinct class of unstable equilibria with tip splitting (and bilateral symmetry) instead of twist.

We then consider how the equilibrium configuration varies with the power law of decay, for an open line of connected charges. We find that stable equilibria are spiral-like for all power laws. For small confinement, faster-decaying power laws lead to tighter spirals. As the radius of the confining sphere decreases, equilibria converge to a common spiral with uniform spacing between turns. However, we find that multiple stable equilibria (all spiral-like) are possible for slowly decaying power laws.

II. THE MODEL

We consider a closed chain (or ring) of n Coulomb charges, connected by linear springs, and lying in a spherically-symmetric potential. The energy of the system is

$$E = \sum_{i=1}^{n} C_1 n (r_{i,i+1} - d)^2 + \sum_{i=1}^{n} \sum_{j=i+1}^{n} \frac{C_2}{n^2 \ln n} \frac{1}{r_{i,j}^p} + \sum_{i=1}^{n} \frac{C_3}{n} \left(e^{[(r_i/R)^2 - 1]/\delta} + e^{-[(r_i/R)^2 - 1]/\delta} \right). \quad (1)$$

The first term is the stretching energy, with spring stiffness $C_1 n$ and equilibrium spring length $d = 2\pi/n$. The length of the chain is thus fixed at 2π, which sets the length scale of the problem. The distance between charge i and charge j is $r_{i,j}$, and indexing is periodic so $n+1=1$. The second term is the generalized Coulomb energy, with charge interaction strength $C_2/n^2 \ln n$ and exponent $p > 0$. The Coulomb interaction tends to drive charges apart, against the stretching interaction which tends to keep neighboring charges at distance d. The third term is the spherical barrier potential. For fixed C_1 and C_2, we take the limit that C_3 is sufficiently large and δ sufficiently small that the charged line lies on the

*alben@math.gatech.edu

sphere of radius R. The factors of n in Eq. (1) are included so that E tends to a finite limit as $n\to\infty$, in the portion of parameter space of interest here, namely, that the configuration of charges tends to a line on the sphere of uniform charge density as $n\to\infty$. We scale the energy in Eq. (1) by C_1, and let $p_2=C_2/C_1$, which leaves p, p_2, and R as the important parameters in the problem.

We now attempt a partial classification of the equilibria as a function of p_2 and R, first restricting to the Coulomb case $p=1$. We consider other p later in this work. If the charge strength is much stronger than the spring stiffness ($p_2\gg 1$), we obtain the classical Thompson problem of unlinked charges on the sphere [12]. In this case, the number of equilibrium states is conjectured to grow exponentially with n [14,18]. Addition of the spring energy greatly reduces the number of equilibria, as we describe below. If the charge strength p_2 is zero, there is a continuum of equilibria consisting of "floppy" chains on the sphere with links of length d. If $R\geqslant 1$, one such chain is a circle of radius 1 on the sphere. If we now set the charge strength p_2 to any positive number, the circle is the unique least-energy state among the floppy chains, because it maximizes the pairwise distances between charges and therefore minimizes the Coulomb energy. We focus on the case where p_2 is positive but sufficiently small that the maximum stretching strain $\max_i\{r_{i,i+1}/d-1\}\ll 1$, so that the chain links are approximately unstretched. A conservative upper bound on such p_2 is obtained by considering one chain link in isolation, and computing the strain ϵ by balancing the stretching and Coulomb forces which arise from the energy in Eq. (1). We obtain $\epsilon=p_2/(2\pi n^2\ln n)$. Thus, if $n>10$ (here $n\geqslant 200$), a strain of less than 1% is obtained for $0<p_2<1$. In fact, the strain in a closed chain is considerably smaller than this estimate, because in the complete chain the Coulomb force on a point charge from one neighbor is nearly cancelled by the other neighbor to the extent that the neighbors lie in a straight line. We therefore begin by setting $p_2=1$, so that we have small strain, and vary R. To simulate a line of uniform charge density, we take n sufficiently large ($n\geqslant 200$) that the spacing between charges is always much smaller than the radius of the sphere. Furthermore, all numerical results given do not change (to the precision given) as n is increased by a factor of 4.

III. THE FIRST BIFURCATION: $k=2$ MODE

For $R\geqslant 1$, the unique equilibrium is a circle of radius 1 on the sphere. We now ask what happens when R is decreased from 1, so that for a chain of length 2π confined to the sphere, a circle is no longer possible. For R slightly less than 1, or $0<(1-R)\ll 1$, we use a perturbation analysis to predict the shape, assuming as a base state the circle $(x,y,z)=(\cos\theta,\sin\theta,0)$. When R is decreased, confinement to a sphere requires the circle to buckle into the z dimension to maintain its length. Figure 1 shows some of the equilibria for $p_2=1$, and R decreasing from 1 to 0.9. At each R in this range the equilibrium is unique. The z deformation assumes a shape with dominant Fourier mode $k=2$. We can understand why the $k=2$ mode appears by considering a general z deformation of wave number k, of the form $z=\epsilon\sin k\theta$. We

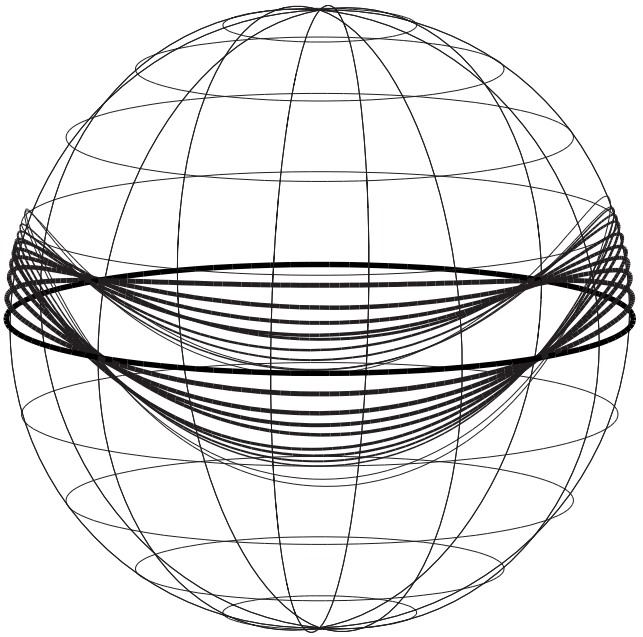

FIG. 1. The charged line equilibria for $0.9<R\leqslant 1$. The horizontal equator is the solution for $R=1$.

determine x and y corresponding to this z by requiring the line to lie on a sphere of radius R: $x^2+y^2+z^2=R^2$, and to be unstretched: $x'^2+y'^2+z'^2=1$, where primes denote differentiation by θ. This provides two equations for the two unknowns x and y. We solve them by expanding x and y in Fourier series and matching coefficients at each wave number and each power of ϵ.

First, the $k=1$ case is degenerate, and corresponds to a rigid body rotation. More precisely, adding $z=\epsilon\sin\theta$ to the base state results in an ellipse in a plane rotated about the x axis. The ellipse can be reduced to a circle of radius 1 by an $O(\epsilon^2)$ addition to y. Modes higher than $k=1$ must then be superposed to yield a closed arc on the sphere of radius R. We can thus obtain the same solution, up to a rotation, by considering only $k\geqslant 2$. For $k\geqslant 2$ the perturbation solutions are

$$x(\theta)=\left(1-\frac{\epsilon^2k^2}{4}\right)\cos\theta+\epsilon^2\frac{2k+5}{16k}\cos(2k-1)\theta+\epsilon^2\frac{2k-5}{16k}\cos(2k+1)\theta+O(\epsilon^4),$$

$$y(\theta)=\left(1-\frac{\epsilon^2k^2}{4}\right)\sin\theta-\epsilon^2\frac{2k+5}{16k}\sin(2k-1)\theta+\epsilon^2\frac{2k-5}{16k}\sin(2k+1)\theta+O(\epsilon^4),$$

$$z=\epsilon\sin k\theta+O(\epsilon^3),$$

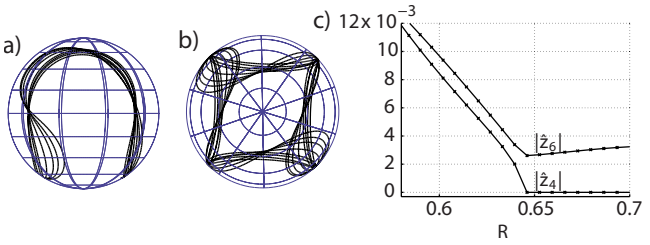

FIG. 2. (Color online) (a) Side view of the equilibrium for R ranging from 0.58 to 0.72, passing through $R_{cr}=0.64$. (b) Top view of the shapes in (a). (c) Magnitude of the $e^{i4\theta}$ and $e^{i6\theta}$ modes in z near R_{cr}.

$$\epsilon^2 = \frac{2}{k^2-1}(1-R^2). \tag{2}$$

The last equation, relating ϵ and R, comes from matching the constant terms in the Fourier series. The inverse relationship between ϵ and wave number k results from conservation of length. Among all such deformations, we evaluate the Coulomb energy in Eq. (1), and find that the $O(1-R^2)$ term in increases monotonely with k. Hence the lowest energy mode is $k=2$.

An intuitive reason is that among all k, the longest-wavelength $k=2$ mode gives the largest distance between a given charge and its next-to-nearest neighbors, by making them fall most nearly along a straight line (ignoring the nearest neighbors, which are always at fixed distance from a given charge).

As $1-R$ becomes larger than infinitessimal, the deformation continues to have a dominant $k=2$ mode, but other modes gradually increase in amplitude to become of the same order as the $k=2$ mode. In Fig. 1 it can be seen that the shapes have two orthogonal planes of symmetry, given here by $\{\theta=\pm\pi/2\}$ and $\{\theta=0,\pi\}$, so that $\mathbf{x}(\pi/2-\theta)=\mathbf{x}(\theta)$. This symmetry holds for all R above a critical radius R_{cr}, and in this regime $z(\theta)$ consists of modes $\{\sin(4k+2)\theta, k\in\mathbb{N}\}$. We now describe the appearance of the modes $\{\sin(4k)\theta, k\in\mathbb{N}\}$ in a second bifurcation.

IV. THE SECOND BIFURCATION: TWIST

As the $k=2$ mode in the z deformation grows, members of the pair of peaks and members of the pair of troughs on the ring in Fig. 1 approach one another. The Coulomb repulsion between the regions about these points increases, which makes other modes more favorable when R drops below a critical value, which is $R_{cr}=0.64$. Below R_{cr}, the $4k$ modes appear in a sharp bifurcation. In Fig. 2(c), we plot the $k=4$ and $k=6$ mode amplitudes at the bifurcation. The $k=4$ mode corresponds to a twisting perturbation, as shown in Figs. 2(a) and 2(b). This twisting perturbation corresponds to the growth of all even modes, although the Fourier spectrum decays exponentially with wave number, as for any smooth periodic curve. The odd modes remain zero, because the shape is doubly periodic. The twisting motion has the effect of slowing the decrease in normal distance between the approaching opposite pairs in the $k=2$ mode.

V. EQUILIBRIA UNDER LARGE DEFORMATIONS

Subsequent decrease of R leads to a continued twisting of the twisted equilibrium shape into a spiral configuration, shown in Fig. 3. Next to the spheres we replot the shapes in a flattened projection in terms of the azimuthal angle $\theta=\arctan(y/x)$ and the polar angle $\phi=\arccos(z/\sqrt{x^2+y^2})$. This equal-area projection is called the sinusoidal projection, or alternatively the "Sanson-Flamsteed projection" or "Mercator projection" [19]. These spiral configurations have approximately uniform distance between turns of the spiral. They are similar to the configurations found by Slosar and Podgornik for the open line [15]. They conjectured a relationship between their spiral configuration and the spiral configurations which arise in the work by Saff and Kuijlaars [17] in determining the minimum energy configuration of interacting points (rather than lines) on a sphere.

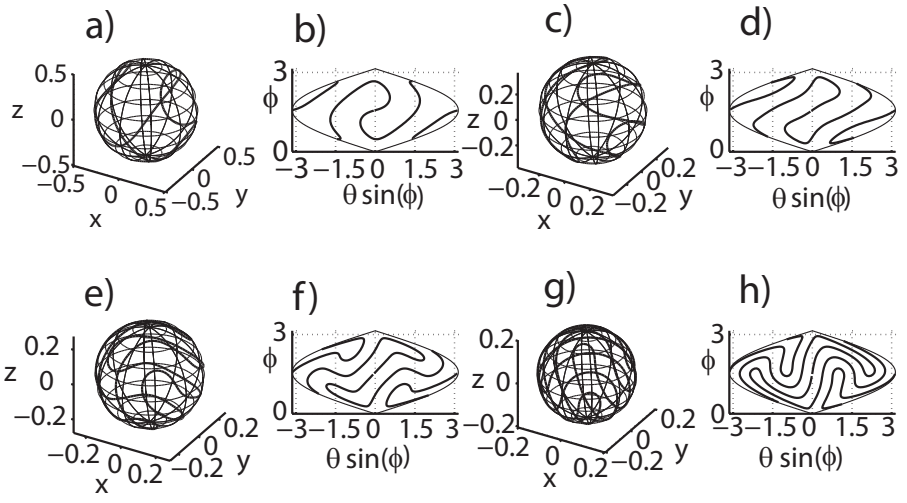

FIG. 3. "Spiral" equilibria of the closed line for R decreasing: $R=0.497$ (a),(b); $R=0.367$ (c),(d); $R=0.271$ (e),(f); $R=0.2$ (g),(h). The panels (b), (d), (f), (h), to the right of the spheres, are flat projections in terms of the azimuthal angle θ and polar angle ϕ.

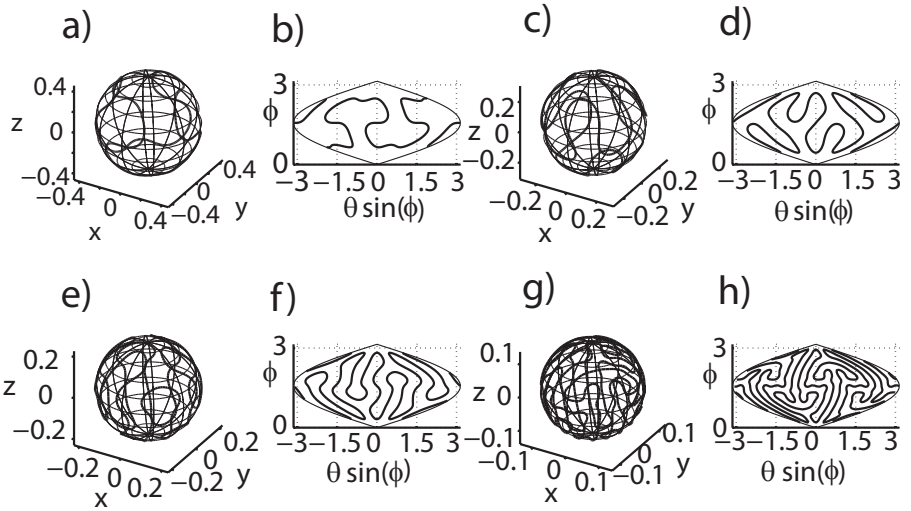

FIG. 4. Unstable "tip-splitting" equilibria of the closed line, for R decreasing: $R=0.45$ (a),(b); $R=0.301$ (c),(d); $R=0.222$ (e),(f); $R=0.134$ (g),(h). The panels (b), (d), (f), (h), to the right of the spheres, are flat projections in terms of the azimuthal angle θ and polar angle ϕ.

The spiral equilibrium is the only stable equilibrium among a number of different equilibria we have obtained by applying (random) perturbations in position to the initial guess for $\mathbf{x}$ at each R, ranging in magnitude from 10^{-1} to 10^{-5}. A branch of unstable equilibria also arises. These states are shown in Fig. 4, and consist of a tip-splitting motion and the absence of the $4k$ modes. The value of R_{cr} at which the first tip splitting occurs is the same as that for the twisting bifurcation. Again, the repulsion between near neighbors favors a long wavelength deformation. The twisting ($k=4$) mode is thus favored over the tip-splitting ($k=6$) mode, though the difference in energy between the two is very small. The tip-splitting mode always arises in numerical simulations with noise below a threshold value, while the spiral mode arises with noise above this value. Equilibria with combinations of tip-splitting states different from that of Fig. 4 have also been observed. None of these modes has twist, and all are apparently unstable, meaning that the Hessian matrix of the energy has negative eigenvalues for these states.

VI. EQUILIBRIA OF AN OPEN LINE

These symmetric unstable equilibria are eliminated when we consider the problem of an open line segment of uniform charge density on the sphere. Here when R is larger than 2, the unique equilibrium is an arc of a great circle on the sphere. As R decreases below 2, the arc gradually transitions to a spiral shape. The number of turns in the spiral increases as R decreases further. A sequence of equilibria for $p=1$ is shown in Fig. 5. The shape of the open line at the end points is of interest. For $p=1$, the electric field near the ends of an open line of uniform charge diverges as the inverse of distance to the end, which is the same divergence as near an

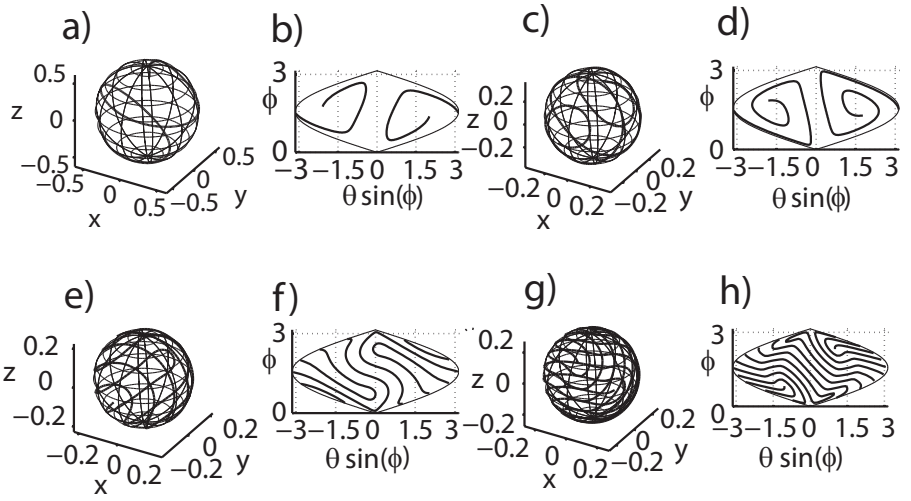

FIG. 5. Sequence of spiral equilibria for the open charged line, with $p=1$, for R decreasing: $R=0.61$ (a),(b); $R=0.368$ (c),(d); $R=0.222$ (e),(f); $R=0.134$ (g),(h). The panels (b), (d), (f), (h), to the right of the spheres, are flat projections in terms of the azimuthal angle θ and polar angle ϕ.

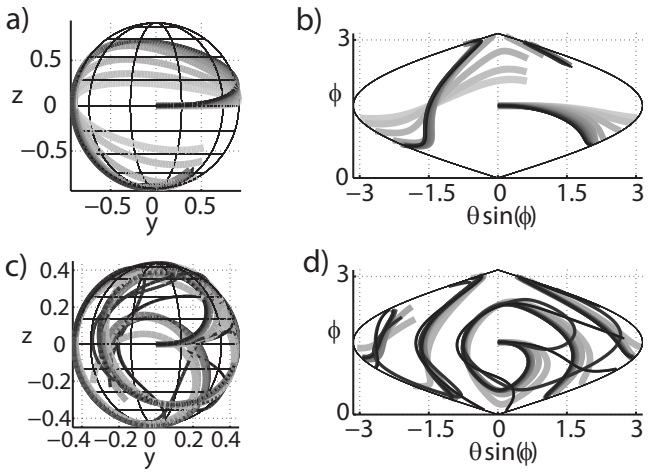

FIG. 6. Comparison of equilibria for $p=0.05$, 0.07, 0.1, 0.2, 0.3, 0.5, 0.7, 1, 1.5, 2, 3, and 4 at $R=0.913$ (a),(b) and 0.437 (c),(d). The lines vary in thickness and shades of grey, where larger p corresponds to greater thickness and lighter shade of gray.

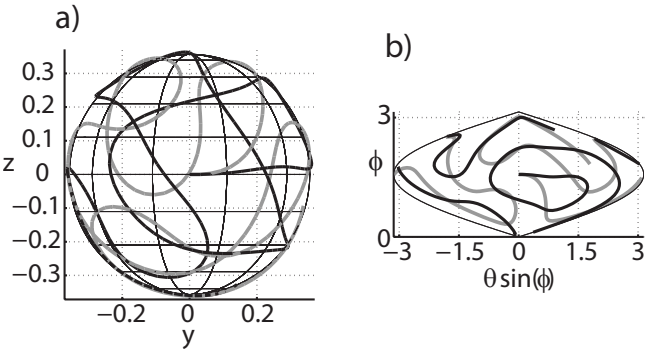

FIG. 7. Two distinct stable equilibria for $R=0.357$ and $p=0.05$. Panel (b) is a flat projection of (a) in terms of the azimuthal angle θ and polar angle ϕ.

interior point. For a continuous line of charge, the prefactor of the divergence for an end point is half that for an interior point, so that there is somewhat less repulsion near the ends. In Fig. 5 we see that the spacing between turns of the spiral becomes smaller near the end points.

VII. OTHER POWER-LAW POTENTIALS

The conformations of DNA or RNA are modified by the presence of a solvent [5]. Different potentials have been used to model charged polymers in solvents, with exponential and power law decay with varying exponents [6]. Here we consider how the conformations of the charged open line vary with respect to the exponent p of power law decay in Eq. (1). In the limit $p\to\infty$, the energy of a charge is dominated by that of its nearest neighbors, which are always at a fixed distance. Thus all conformations have the same leading-order divergent term in their energies in this limit. In the limit $p\to 0$, the energy becomes independent of the distance between charges, so again all conformations have the same energy. (Negative p gives an attractive potential.) For intermediate p, however, there are well-defined equilibria which vary with p.

In Fig. 6 we plot the conformations for p varying over two orders of magnitude at two different values of R. For the larger $R=0.913$, the larger p have somewhat tighter spirals. Due to the faster decay of the repulsion, the end points of the open line do not repel each other as strongly, and it is this repulsion that leads to the initial transition from an arc of a great circle into a spiral. At the smaller $R=0.437$, many of the lines have nearly converged to a spiral similar to others we have encountered so far, one with nearly uniform spacing between neighboring turns. At smaller p we find different conformations, but with a similar spacing between neighboring turns, as is evident in Fig. 6(d). Unlike at $R=0.913$, here all points of the open line are nearly equidistant from adjacent but noncontiguous regions of the line. Apparently any repulsion is sufficient to create such a spiral state once the packing density is sufficiently high (or R, which is an inverse packing density, is sufficiently low).

In Fig. 7 we show that multiple stable equilibria are possible for the open line with sufficiently small p. We give examples of two stable equilibria for $p=0.05$, found by adding different random perturbations during the minimization search procedure. Both states give spirals with nearly uniform spacing between neighboring turns. The orientation of the turns varies differently between the two states over the sphere. The amount of curvature near the open ends is also different between the two states. All of the spirals we have discussed have two opposite "poles" where the curvature is largest. The placement of the open ends within the spiral is not precisely determined, however. There is also the possibility of some variation in the configuration of the windings of the spiral as the sphere is traversed, somewhat similar to the global disordered configurations identified by Ref. [16].

VIII. CONCLUSION

We have considered the problem of the equilibria of a line of uniform charge confined to the surface of a sphere, as a function of the radius of the sphere. For a closed line, we have identified the sequence of bifurcations which leads to the eventual, apparently unique, stable equilibrium of a spiral configuration. The first bifurcation is from an equatorial circle into a $k=2$ mode of deflection out of the plane of the circle. The second bifurcation is the loss of bilateral symmetry in the form of twist. Further development leads to a spiral of an increasing number of turns with approximately uniform spacing. We also identify unstable equilibria consisting of tip-splitting events, reminiscent of fingering phenomena in fluid dynamics (though the physical mechanism is different). The open line of charge, by contrast, has a simpler transition from an arc of a great circle into a spiral configuration as R decreases. We have also examined the effect of varying the power law of repulsion. Faster decay leads initially to tighter spirals, but as R decreases below $1/2$, the different power law spirals converge to a class of spirals with uniform spacing between turns. We have identified multiple stable equilibria for slowly decaying repulsion $p\leqslant 0.05$.

[1] I. Ali, D. Marenduzzo, and J. M. Yeomans, J. Chem. Phys. **121**, 8635 (2004).
[2] J. U. Bowie, Nature (London) **438** 581 (2005).
[3] B. V. Velamakanni, J. C. Chang, F. F. Lange, and D. S. Pearson, Langmuir **6**, 1323 (1990).
[4] C. Steven, Biopolymers **17**, 794 (1978).
[5] A. S. Petrov and S. C. Harvey, Structure (London) **15**, 21 (2007).
[6] R. L. Ricca and F. Maggioni, Comput. Math. Appl. **55**, 1044 (2008).
[7] C. Petit, A. Taleb, and M. P. Pileni, Adv. Mater. (Weinheim, Ger.) **10**, 259 (1998).
[8] C. Li, X. Zhang, and Z. Cao, Science **309**, 909 (2005).
[9] S. L. Tripp, S. V. Pusztay, A. E. Ribbe, and A. Wei, J. Am. Chem. Soc. **124**, 7914 (2002).
[10] B. A. Grzybowski, X. Jiang, H. A. Stone, and G. M. Whitesides, Phys. Rev. E **64**, 011603 (2001).
[11] M. Klokkenburg, R. P. A. Dullens, W. K. Kegel, B. H. Erné, and A. P. Philipse, Phys. Rev. Lett. **96**, 037203 (2006).
[12] J. J. Thomson, Philos. Mag. **7**, 237 (1904).
[13] M. J. Bowick, A. Cacciuto, D. R. Nelson, and A. Travesset, Phys. Rev. B **73**, 024115 (2006).
[14] E. L. Altschuler, T. J. Williams, E. R. Ratner, R. Tipton, R. Stong, F. Dowla, and F. Wooten, Phys. Rev. Lett. **78**, 2681 (1997).
[15] A. Slosar and R. Podgornik, Europhys. Lett. **75**, 631 (2006).
[16] D. G. Angelescu, P. Linse, T. T. Nguyen, and R. F. Bruinsma, Eur. Phys. J. E **25**, 323 (2008).
[17] E. B. Saff and A. B. J. Kuijlaars, Math. Intell. **19**, 5 (1997).
[18] D. J. Wales and S. Ulker, Phys. Rev. B **74**, 212101 (2006).
[19] L. M. Bugayevskiy and J. P. Snyder, *Map Projections: A Reference Manual* (Taylor & Francis, New York, 1995).